

# Traveling wave packets of total electron content disturbances as deduced from global GPS network data

Afraimovich E. L., Perevalova N. P., Voeikov S. V.

## Abstract

We identified a new class of mid-latitude medium-scale traveling ionospheric disturbances (MS TIDs), viz. traveling wave packets (TWPs) of total electron content (TEC) disturbances. For the first time, the morphology of TWPs is presented for 105 days from the time interval 1998-2001 with a different level of geomagnetic activity, with the number of stations of the global GPS network ranging from 10 to 300. The radio paths used in the analysis total about 700000. These data were obtained using the GLOBDET technology for global detection and monitoring of ionospheric disturbances of natural and technogenic origin from measurements of TEC variations acquired by a global network of receivers of the navigation GPS system. The GLOBDET technology was developed at the ISTP SB RAS. Using the technique of GPS interferometry of TIDs we carried out a detailed analysis of the spatial-temporal properties of TWPs by considering an example of the most conspicuous manifestation of TWPs on October 18, 2001 over California, USA. It was found that TWPs are observed no more than in 0.1-0.4% of all radio paths, most commonly during the daytime in winter and autumn at low geomagnetic activity. TWPs in the time range represent quasi-periodic oscillations of TEC of a length on the order of 1 hour with the oscillation period in the range 10-20 min and the amplitude exceeding the amplitude of "background" TEC fluctuations by one order of magnitude, as a minimum. The radius of spatial correlation of TWPs does not exceed 500-600 km (3-5 wavelengths). The velocity and direction of TWPs correspond to those of mid-latitude medium-scale traveling ionospheric disturbances (MS TIDs) obtained previously from analyzing the phase characteristics of

HF radio signals as well as signals from geostationary satellites and discrete cosmic radio sources.

## 1 Introduction

The unremitting interest in investigations of atmospheric acoustic-gravity waves (AGW) over more than four decades dating back to Hines pioneering work (Hines, 1960, 1967) is dictated by the important role played by these waves in the dynamics of the Earth's atmosphere. These research efforts have been addressed in a large number of publications, including a series of through reviews (Hocke and Schlegel, 1996; Oliver et al., 1997).

AGW typically show up in the ionosphere in the form of traveling ionospheric disturbances (TIDs) and are detected by various radio techniques. TIDs are classified as large- and medium-scale disturbances differing by their horizontal phase velocity which is larger (in the large-scale case) or smaller (for the medium scale) velocity of sound in the lower thermosphere (on the order of 300 m/s), with periods within 0.5–3.0 h and 10–40 min, respectively. Medium-scale TIDs (MS TIDs) are observed predominantly during the day-time hours and are associated with AGW which are generated in the lower atmosphere. Large-scale TIDs are predominant in the night-time hours and are closely associated with geomagnetic and auroral activity.

It is known that the sources of medium-scale AGW can include natural processes of a different origin: magnetic storms, auroral phenomena, weather factors, tropospheric turbulence and jet flows, the solar terminator, strong earthquakes, volcanic eruptions, as well as anthropogenic influences (rocket launchings, explosions, nuclear tests). As a consequence the observed picture of the electron density disturbance is essentially a net interference wave field of the AGW of a different origin. Identifying of the AGW of a definite type from this field is a highly involved and generally an almost intractable problem.

The most reliable measurements of the main parameters of medium-scale AGW (parameters of the wave vector of the AGW, spectral and dispersion characteristics, etc.) can therefore be made only for a very rare, unusual type of MS TIDs, i.e. quasi-periodic (monochromatic) oscillations which are sometimes recorded as corresponding variations of the frequency Doppler shift  $F_D$  of the ionosphere-reflected HF radio signal (Davies and Jones, 1971;

Waldock and Jones, 1987; Jacobson and Carlos, 1991; Yakovets et al., 1999).

Experiments of this kind were instrumental in investigating the spatial-temporal characteristics of MS TIDs in the form of a wave process, because such recordings are easy to identify visually with monochromatic individual AGW. Unfortunately, this was possible to accomplish for a very limited body of experimental data. Thus, Jacobson and Carlos (1991) managed to identify only a few monochromatic TIDs from their data obtained for more than 100 hours of observation.

Yakovets et al. (1999) also recorded only a few realizations of monochromatic TIDs for two observing periods from the winter months of 1989 and 1990. Yakovets et al. (1999) are likely to be the first to use the term "wave packets" to designate the quasi-monochromatic variations of  $F_D$ , and they made an attempt to explain their origin on the basis of studying the phase structure of the oscillations. The authors of the cited reference observed two types of  $F_D$ -variations: quasi-stochastic TIDs, and monochromatic TIDs in the form of wave packets. They arrived at the conclusion that quasi-stochastic TIDs are characterized by a random phase behavior, a short length of coherence, and by a large vertical phase velocity. Wave packets show quasi-monochromatic oscillations of  $F_D$ , a larger length of coherence, and a smaller vertical phase velocity.

Following Yakovets et al. (1999), we chose to utilize the term "wave packets" by expanding it to the term "traveling wave packets" (TWPs). The investigation made in this paper has brought out clearly that this designation describes most adequately the phenomenon involved.

Some authors associate the variations of the frequency Doppler shift  $F_D$  with MS TIDs that are generated during the passage of atmospheric fronts, tornadoes, and hurricanes (Baker and Davies, 1969; Bertin et al., 1975; 1978; Hung et al., 1978; Kersly and Rees, 1982; Stobie et al., 1983; Huang et al., 1985). It is only in some cases that these experiments observed quasi-monochromatic variations of  $F_D$  with periods of about 10 min (Huang et al., 1985).

Thus, in spite of the many years of experimental and theoretical studied, so far there is no clear understanding not only of the physical origin of the quasi-monochromatic MS TIDs but even of their morphology as well (the occurrence frequency as a function of geographical location, time, level of geomagnetic and meteorological activity, etc.).

To address these issues requires obtaining statistically significant sets of

experimental data with good spatial resolution in order to study not only the morphological but also dynamic characteristics of quasi-monochromatic MS TIDs (the direction of their displacement, their propagation velocity, and the location of the possible disturbance source). Another important requirement implies the continuous, global character of observations, because such phenomena are temporally highly rare and spatially random.

Such a possibility is, for the first time, afforded by the use of the international ground-based network of two-frequency receivers of the navigation GPS system which at the beginning of 2002 consisted of no less than 1000 sites, with its data posted on the Internet, which opens up a new era of a global, continuous and fully computerized monitoring of ionospheric disturbances of a different class. Analysis and identification of TWPs became possible through the use of the technology (developed at the ISTP) for global detection and determination of parameters of ionospheric disturbances of a different class.

The objective of this paper is to study the morphology and spatial-temporal properties of TWPs using the data from the global network of GPS receivers. Section 2 provides general information about the experiment and gives a brief description of the method of TWPs detecting. Section 3 presents our new evidence characterizing the TWPs morphology. Section 4 is devoted to a detailed analysis of the spatial-temporal properties of TWPs by considering an example of the most pronounced manifestation of TWPs on October 18, 2001 as observed in California, USA. The discussion of our results compared with the findings reported by other authors is given in Section 5.

## **2 General information about the experiment and method of TWPs detecting**

This paper presents, for the first time, the morphology of TWPs for 105 days of 1998–2001, with a different level of geomagnetic activity and with the number of stations of the global GPS network ranging from 10 to 300. A total number of the TEC series used in the analysis, corresponding to the observation along a single receiver-satellite Line-of-Sight (LOS), with a duration of each series of about 2.3 hours, exceeded 700000.

For a diversity of reasons, slightly differing sets of GPS stations were selected for different events to be analyzed; however, the geometry of experiment for all events was virtually identical. The stations coordinates are not given here for reasons of space. This information may be found at the electronic address <http://lox.ucsd.edu/cgi-bin/allCoords.cgi?>. The global GPS covers rather densely North America and Europe, and to a much lesser extent Asia. GPS stations are more sparsely distributed on the Pacific and Atlantic Oceans. However, such coverage of the surface of the globe makes it possible, already today, to tackle the problem of global detection of disturbances with hitherto unprecedented spatial accumulation. Thus, in the Western hemisphere the corresponding number of stations can reach no less than 500 already today, and the number of LOS to the satellite can be no less than 2000–3000.

The area of California, USA, is particularly convenient for our investigations because of the large number of GPS stations (no less than 300) located over a relatively small area, which makes it possible to obtain a great variety of GPS arrays of a different configuration for a reliable determination of the dynamic TWP parameters using the method of GPS interferometry of TIDs (Afraimovich et al., 1998; 2000).

The comparison of TWP characteristics with geomagnetic field variations was based on using the data from the INTERMAGNET network (INTERMAGNET, <http://www.intermagnet.org/>).

## 2.1 Method of processing the data from the global network. Selection of TWPs

The standard GPS technology provides a means for wave disturbances detection based on phase measurements of TEC  $I_0$  (Hofmann-Wellenhof et al., 1992):

$$I_0 = \frac{1}{40.308} \frac{f_1^2 f_2^2}{f_1^2 - f_2^2} [(L_1 \lambda_1 - L_2 \lambda_2) + const + nL] \quad (1)$$

where  $L_1 \lambda_1$  and  $L_2 \lambda_2$  are additional paths of the radio signal caused by the phase delay in the ionosphere, (m);  $L_1$  and  $L_2$  represent the number of phase rotations at the frequencies  $f_1$  and  $f_2$ ;  $\lambda_1$  and  $\lambda_2$  stand for the corresponding wavelengths, (m); *const* is the unknown initial phase ambiguity, (m); and

$nL$  are errors in determining the phase path, (m).

Phase measurements in the GPS can be made with a high degree of accuracy corresponding to the error of TEC determination of at least  $10^{14}$   $\text{m}^{-2}$  when averaged on a 30-second time interval, with some uncertainty of the initial value of TEC, however (Hofmann-Wellenhof et al., 1992). This makes possible detecting ionization irregularities and wave processes in the ionosphere over a wide range of amplitudes (up to  $10^{-4}$  of the diurnal TEC variation) and periods (from 24 hours to 5 min). The unit of TEC, which is equal to  $10^{16}$   $\text{m}^{-2}$  (*TECU*) and is commonly accepted in the literature, will be used in the following.

In some instances a convenient way for comparing TEC response characteristics from the GPS data with those obtained by analyzing the frequency Doppler shift in the HF range (Davies and Jones, 1971; Waldock and Jones, 1987; Jacobson and Carlos, 1991; Yakovets et al., 1999) is to estimate the frequency Doppler shift  $F_D$  from TEC series obtained by formula (1). To an approximation sufficient for the purpose of our investigation, a corresponding relationship was obtained by (Davies, 1969):

$$F_D = 13.5 \times 10^{-8} I'_t / f \quad (2)$$

where  $I'_t$  stands for the time derivative of TEC.

Primary data include series of "oblique" values of TEC  $I_0(t)$ , as well as the corresponding series of elevations  $\theta(t)$  and azimuths  $\alpha(t)$  along LOS to the satellite calculated using our developed CONVTEC program which converts the GPS system standard RINEX-files on the INTERNET (Gurtner, 1993). For TWP's characteristics to be determined continuous series of  $I_0(t)$  series of a duration of no less than 2.3 hours are chosen.

To normalize the response amplitude we converted the "oblique" TEC to an equivalent "vertical" value (Klobuchar, 1986):

$$I = I_0 \times \cos \left[ \arcsin \left( \frac{R_z}{R_z + h_{max}} \cos \theta \right) \right], \quad (3)$$

where  $R_z$  is the Earth's radius, and  $h_{max} = 300$  km is the height of the  $F_2$ -layer maximum.

The most reliable results from the determination of TWP's parameters correspond to high values of elevations  $\theta(t)$  of the beam to the satellite because sphericity effects become reasonably small. All results in this study

were obtained for elevations  $\theta(t)$  larger than  $30^\circ$ .

To exclude the variations of the regular ionosphere, as well as trends introduced by the motion of the satellite, we employ the procedure of removing the linear trend by preliminarily smoothing the initial series with a convenient time window.

The technology for global detection of TWPs that was developed at the ISTP SB RAS makes it possible to select – from a large amount of experimental material in the automatic mode – the TEC disturbances which can be assigned to a class of TWPs.

The selection of TEC series which could be ascribed to a class of TWPs was carried out by two criteria (Fig. 1). First of all, TEC variations were selected, for which the value of the standard deviation exceeded a given threshold  $\epsilon$  (in the present case  $\epsilon = 0.1 \text{ TECU}$ ).

In addition, for each filtered series, we verified the fulfillment of the "quasi-monochromaticity" condition of TEC oscillations, for which the ratio  $R$  of a total spectral signal power in the selected frequency band  $\delta F$  in the neighborhood of a maximum value of the power  $S_{max}$ , to a total spectral signal power outside the frequency band  $\delta F$  under consideration exceeded a given threshold  $R_{min}$  (in the present case  $R_{min} = 2$ ).

Fig. 1 illustrates the selection process of the TWPs. Fig. 1a gives an example of weakly disturbed variations of the "vertical" TEC  $I(t)$  as recorded on July 15, 2001 at station DARW ( $131.13^\circ\text{E}$ ;  $12.8^\circ\text{S}$ ; satellite number PRN05). Fig. 1b presents the  $dI(t)$ -variations that were filtered from the initial  $I(t)$ -series. Thin horizontal lines show the specified threshold  $\epsilon$ . The standard deviation of the  $dI(t)$ -variations is  $0.019 \text{ TECU}$ , that is, does not reach the specified threshold  $\epsilon = 0.1 \text{ TECU}$ .

Fig. 1c illustrates the  $S(F)$  spectrum of the series  $dI(t)$  from Fig. 1b. Thin vertical lines show the boundaries of the frequency range  $\delta F$ . For this spectrum  $R = 0.66$  is smaller than the specified  $R_{min} = 2$  and, hence, the series  $dI(t)$  does not satisfy the condition of "quasi-monochromaticity".

Fig. 1d, 1e and 1f plots the same dependencies as in Fig. 1a, 1b and 1c but for station TOW2 ( $147^\circ\text{E}$ ;  $19.3^\circ\text{S}$ ; satellite number PRN09). It is evident from Fig. 1d that at the background of the slow TEC variations there are clearly identifiable (unusual for background TEC disturbances) oscillations in the form of a wave packet of a duration of about 1 hour and with a typical period  $T$  in the range from 10 to 18 min. The oscillation amplitude of the detected wave packet exceeds one order of magnitude (as

a minimum) the intensity of background TEC fluctuations of this range of periods (Afraimovich et al., 2001a).

The relative amplitude of such a response  $\Delta I/I_0$  is considerable, 4 %. As the background value of  $I_0$  we used the absolute "vertical" TEC value of  $I_0(t)$  for the site located at 19.3°S; 147°E, obtained from IONEX TEC maps (Mannucci, 1998). Since the main contribution to the modulation of the TEC is made by the region near the ionospheric  $F$ -region peak, the relative amplitude of the local electron density disturbance  $\Delta N/N_0$  in this region can be several times larger than  $\Delta I/I_0$ .

It is worthwhile to note that the two examples described above refer to the same time interval and to the stations spaced by a distance of no more than 1900 km from one another. This suggests a local character of the phenomenon and is in agreement with the overall sample statistic characterizing its spatial correlation (see below).

The standard deviation of the series  $dI(t)$ , shown in Fig. 1e, is 0.114  $TECU$ , which is larger than the specified threshold  $\epsilon=0.1$   $TECU$ , and this series satisfies the condition for the standard deviation. Fig. 1f presents the spectrum  $S(F)$  of the series  $dI(t)$ , shown in Fig. 1e. For this spectrum  $R = 3.71$ , which is larger than the specified  $R_{min} = 2$ , that is, in this case the series  $dI(t)$  satisfies the condition of "quasi-monochromaticity".

Panel e shows the maximum value of the amplitude  $A_{max}$  of the packet and the time  $t_{max}$  corresponding to this amplitude.

When the filtered  $dI(t)$ -series satisfied the conditions described above, such an event was recognized as TWP.

Furthermore, for each such event, a special file stored information about the name, geographical latitude  $\phi_s$  and longitude  $\lambda_s$  of the GPS station; the GPS satellite PRN number; the time  $t_{max}$  corresponding to the maximum value of the amplitude  $A_{max}$  of the TWP; the amplitude  $A_{max}$ ; the TWP oscillation period  $T$ ; the  $R$  ratio; and about the value of the elevation  $\theta_s(t)$  and the azimuth  $\alpha_s(t)$  of the LOS to the satellite calculated for the time  $t_{max}$ . The sample statistic, presented below, was obtained by processing such files for our selected value of  $\epsilon=0.1$   $TECU$ .



### 3 Morphology of TWPs

The method outlined above was used to obtain a series of TWPs totaling about 1300 cases, or about 0.2% of the total number of the radio paths considered (receiver-satellite LOS). As has been pointed out above, the radio paths that were considered totaled over 700000. An analysis of the resulting statistic revealed a number of dependencies of the TWPs parameters on different factors.

First of all, we consider the seasonal dependence of the density and amplitude of the TWPs (Fig. 2). Fig. 2a plots the dependence of the number of days of observation  $M$  on the time of the year. It is evident that statistically, the autumn season is represented best. Fig. 2b shows the seasonal dependence of the number of TWPs  $N$ . Fig. 2c plots the number of TWPs  $L = N/M$  per day as a function of time of the year. This dependence has maxima in winter and in autumn.

The relative TWPs density  $D$ , obtained as the ratio of the number of TWPs  $N$  to the number of receiver-satellite LOS, is presented in Fig. 2d. As is apparent from the figure, TWPs are observed in no more than 0.1-0.4% of the total number of radio paths, and much more frequently in winter (over 0.4%) and autumn (up to 0.3%) than in spring and summer (less than 0.1%).

Diamonds in Fig. 2d show the mean values of  $\langle A \rangle$  of the maximum TWPs amplitudes  $A_{max}$  for each season, and vertical lines show their standard deviations. Thick horizontal line shows the threshold in amplitude  $\epsilon=0.1 \text{ TECU}$ . The most probable value of  $\langle A \rangle$  with a small scatter varies around the value  $0.3 \text{ TECU}$ , irrespective of the season.

Fig. 3d presents the normalized occurrence probability distribution of TWPs with the specified maximum amplitude of the packet  $A_{max}$ . The vertical dashed line shows the threshold in amplitude  $\epsilon=0.1 \text{ TECU}$ . It was found that the most probable value of the amplitude  $A_m$ , also shown in Fig. 3d, is about  $0.3 \text{ TECU}$ , and the half-width of the distribution is  $0.2 \text{ TECU}$ . As was shown by Afraimovich et al. (2001a), the mean values of the TEC variation amplitude with the period of 20 min for the magnetically quiet and magnetically disturbed days do not exceed  $0.01 \text{ TECU}$  and  $0.07 \text{ TECU}$ , respectively. Thus the most probable value of the amplitude  $A_m$  of TWPs exceeds the mean value of the TEC variation amplitude by a factor of 4–6 as a minimum. This estimate is consistent with the variation amplitude of the frequency Doppler shift  $F_D$  reported by Yakovets et al. (1999).

Fig. 3b presents the diurnal distribution  $P(t_{max})$  of the times  $t_{max}$  corresponding to the maximum value of the amplitude  $A_{max}$  of the wave packet of TWPs. It is evident that most of the TWPs (about 87%) are observed during the daytime, from about 7:00 to 16:00 of local time, LT.

Fig. 3a plots the dependence  $P(|Dst|)$  of the number of TWPs on the values of the geomagnetic activity index  $Dst$  taken by the modulus. There is a general tendency of the number of TWPs to increase with the decreasing level of geomagnetic activity. Most (about 92%) of the TWPs occur when the values of the  $Dst$ -index are smaller than 100 nT.

The availability of a large number of GPS stations in some regions of the globe (in California, USA and West Europe, for example) makes it possible to determine not only the temporal but also spatial characteristics of TWPs. To estimate the radius of spatial correlation of events of this type we calculated the number of cases where the TWPs within a single 2.3-hour time interval were observed at any two GPS stations separated by  $dR$ . Fig. 3c presents the histogram of values of  $P(dR)$  as a function of distance  $dR$ . It was found that the localization of the TWPs in space is strongly pronounced. In 82% of cases the distance  $dR$  does not exceed 500 km.

## 4 Traveling wave packets of total electron content pulsations as deduced from a case study of the October 18, 2001 event

Using the method of GPS interferometry of TIDs (Afraimovich et al., 1998; 2000), we carried out a detailed analysis of the spatial-temporal properties of TWPs by considering an example of the most pronounced manifestation of TWPs on October 18, 2001 over California, USA. Numerous traveling ionospheric disturbances of the type of TWPs were recorded on that day between 15:00 and 18:00 UT using signals from several satellites, at many GPS stations located in California.

## 4.1 Geometry and general information about the October 18, 2001 experiment

The area of California within  $220 - 260^\circ\text{E}$ ;  $28 - 42^\circ\text{N}$  is convenient for our investigations because of a large number of GPS stations located there, which makes it possible to obtain a great variety of GPS arrays of a different configuration for determining the TID parameters and provides a means of verifying the reliability of calculated data. It is also important that for the above-mentioned time interval 15:18 UT and for the chosen longitude range the local time varied from 08 to 11 LT, which reduces the level of background TEC fluctuations characteristic for the night-time.

Fig. 4 illustrates the geometry of the experiment of October 18, 2001. Heavy dots show the GPS stations, and small dots show the position of subionospheric points for GPS receiver-satellite LOS. Since each receiver site observes simultaneously several (no less than four) GPS satellites, the number of radio paths far exceeds the number of stations, which enhances the capabilities of analysis. Fig. 4a presents the entire set of GPS stations used in the experiment. Fig. 4b and 4c show the stations and the subionospheric points where the TEC variations revealed TWPs with an amplitude exceeding the specified threshold  $\epsilon=0.05 \text{ TECU}$  (Fig. 4b) and  $\epsilon=0.1 \text{ TECU}$  (Fig. 4c). With the sole exception, TWPs were recorded along the paths over and, predominantly in the north-eastward direction. As is evident from Fig. 4, an increase of the recording threshold by a factor of two reduced the number of recorded events by a factor of two. Stations shown in Fig. 4c were used as the elements of the GPS arrays in calculating the TWPs parameters.

The geomagnetic situation on October 18, 2001 may be characterized as a weakly disturbed one, which must lead to some increase of the level of background TEC fluctuations yet cannot cause large-scale changes in electron density characteristic for a geomagnetically disturbed ionosphere.

Geomagnetic field  $Dst$ -variations for October 18, 2001 are plotted in Fig. 5a. In the analysis of the geomagnetic situation we used also the data from magnetic observatory Victoria ( $48.52^\circ\text{N}$ ;  $236.58^\circ\text{E}$ ) where for the time interval of our interest a weak geomagnetic disturbance was recorded, which implied a decrease of the horizontal component  $H(t)$  of the magnetic field by 60 nT (Fig. 5b). There was a concurrent, small decrease of the fluctuation amplitude of the  $dH(t)$ -component in the range of periods 2-20 min (Fig. 5c). The range of variation of the geomagnetic  $Dst$ -index for the selected

time interval was also relatively small (no more than 20 nT), yet the period 15:30-18:00 UT showed a clearly pronounced decrease of the  $Dst$ -index coinciding with the period of the decrease of the  $H$ -component of the magnetic field (Fig. 5a).

Fig. 5d presents the distribution  $N(t)$  of the number of TWPs detected for that day by all stations of the global GPS system analyzed here, with the standard deviation in excess of  $\epsilon = 0.1 \text{ TECU}$ . Fig. 5e illustrates the dynamic amplitude spectrum  $S(f, t)$  of TEC variations in the range of periods 5–60 min obtained by using the method of spatial averaging of the spectra for the entire California region (Afraimovich et al., 2001a).

Overall, the TEC variations correlate with geomagnetic field variations. Between 15:00 and 19:00 UT, the enhancement of the oscillations of the  $H$ -component was accompanied by an expansion of the spectrum and by an increase of the TEC fluctuation amplitude. The highest intensity is shown by the TEC oscillations with periods of 12–17 min between 15:30 and 17:00 UT. The largest number of TWPs was also recorded during the same period of time (Fig. 5d).

To check that TWPs were observed on that day somewhere else on the globe and not only between 15 and 19 UT, we processed the data with different values of the threshold  $\epsilon$  for the entire global GPS network.

Fig. 6 presents the sample statistic of the pulsations identified for October 18, 2001 as a function of UT and local time LT, calculated for the longitude of 240°E corresponding to the middle of the California region: Fig. 6a - from TWPs with the standard deviation higher than  $\epsilon = 0.1 \text{ TECU}$  obtained from all stations of the global GPS network used in the study (copy of Fig. 5d); Fig. 6b and Fig. 6c - same as in Fig. 6a but for  $\epsilon = 0.05 \text{ TECU}$  and  $\epsilon = 0.01 \text{ TECU}$ ; Fig. 6d - standard deviation higher than  $\epsilon = 0.01 \text{ TECU}$  for the data from the California region only.

An analysis of the Fig. 6 data leads us to conclude that the TWPs on that day were observed mainly in California only and only over the time interval 15–17 UT.

## 4.2 Methods of determining the form and dynamic characteristics of TWP

The methods of determining the form and dynamic characteristics of TIDs that are used in this study are based on those reported in (Mercier, 1986; Afraimovich, 1995; 1997; Afraimovich et al., 1998; 1999).

We determine the velocity and direction of motion of the phase interference pattern (phase front) in terms of some model of this pattern, an adequate choice of which is of critical importance. In the simplest form, space-time variations in phase of the transionospheric radio signal that are proportional to TEC variations  $I(t, x, y)$  in the ionosphere, at each given time  $t$  can be represented in terms of the phase interference pattern that moves without a change in its shape (the non dispersive disturbances):

$$I(t, x, y) = F(t - x/u_x - y/u_y) \quad (4)$$

where  $u_x(t)$  and  $u_y(t)$  are the velocities of intersection of the phase front of the axes  $x$  (directed to the East) and  $y$  (directed to the North), respectively.

A special case of (4) is the most often used model for a solitary, plane travelling wave of TEC disturbance:

$$I(t, x, y) = \delta \sin(\Omega t - K_x x - K_y y + \varphi_0) \quad (5)$$

where  $I(t, x, y)$  are space-time variations of TEC;  $\delta(t) = \exp[-((t - t_{\max})/(t_d))^2]$  – the amplitude;  $K_x, K_y, \Omega$  are the  $x$ - and  $y$ - projections of the wave vector  $\mathbf{K}$ , and the angular frequency of the disturbance, respectively;  $\varphi_0$  is the initial disturbance phase;  $t_{\max}$  is the time when the disturbance has a maximum amplitude;  $t_d$  is the half-thickness of the 'wave packet'.

It should be noticed, however, that in real situations neither of these ideal models (4), (5) are realized in a pure form. This is because that the AGW that cause TIDs propagate in the atmosphere in the form of a dispersing wave packet with a finite value of the width of the angular spectrum. But in the first approximation on short time interval of averaging compared to time period of filtered variations of TEC, the phase interference pattern moves without a substantial change in its shape.

Mercier (1986) suggested a statistical method to analyze the phase interference pattern. Primary data comprise time dependencies of the spatial phase derivatives  $I'_y(t)$  and  $I'_x(t)$  along the directions  $y$  and  $x$ . Method

Mercier (1986) involves determining a series of instantaneous values of the direction  $\alpha(t)$

$$\alpha(t) = \arctan(I'_x(t)/I'_y(t)) \quad (6)$$

and constructing subsequently, on a chosen time interval, the distribution function of azimuth  $P(\alpha)$ . The central value of  $\alpha$  is used by Mercier as an estimate of the azimuth of prevailing propagation of TIDs (modulo  $180^\circ$ ).

The other method is based on analyzing the phase interference pattern anisotropy in the antenna array plane by determining the contrast  $C$  of the interference pattern (Mercier, 1986). In this case the ratio  $C_{x,y}$  is calculated as follows:

$$\begin{aligned} C_{x,y} &= \sigma_X/\sigma_Y, \quad \text{if } \sigma_X > \sigma_Y \\ C_{x,y} &= \sigma_Y/\sigma_X, \quad \text{if } \sigma_Y > \sigma_X \end{aligned} \quad (7)$$

where  $X$  and  $Y$  are series of the transformed values of  $I'_x(t)$  and  $I'_y(t)$  obtained by rotating the original coordinate system  $(x, y)$  by the angle  $\beta$ :

$$\begin{aligned} X(t) &= I'_x(t) \sin \beta + I'_y(t) \cos \beta \\ Y(t) &= -I'_x(t) \cos \beta + I'_y(t) \sin \beta \end{aligned} \quad (8)$$

and  $\sigma_X$  and  $\sigma_Y$  are r. m. s. of the corresponding series.

Mercier (1986) showed that it is possible to find such a value of the rotation angle  $\beta_0$ , at which the ratio  $C_{x,y}$  will be a maximum and equal to the value of contrast  $C$ . This parameter characterizes the degree of anisotropy of the phase interference pattern. The angle  $\beta_0$  in this case indicates the direction of elongation, and the angle  $\alpha_c = \beta_0 + \pi/2$  indicates the direction of the wave vector  $\mathbf{K}$  coincident (modulo  $180^\circ$ ) with the propagation direction of the phase front.

The method of Mercier (1986) essentially makes it possible to determine only the anisotropy and the direction of irregularity elongation of the phase interference pattern (modulo  $180^\circ$ ).

A Statistical, Angle-of-arrival and Doppler Method (SADM) is proposed by Afraimovich (1995, 1997) for determining characteristics of the dynamics of the phase interference pattern in the horizontal plane by measuring variations of phase derivatives with respect not only to spatial coordinates  $I'_x(t)$  and  $I'_y(t)$  - proportional to the angles of arrival variations, but additionally to time  $I'_t(t)$  - proportional to the frequency Doppler shift variations. This

permits to ascertain the unambiguous orientation of  $\alpha(t)$  of the wave-vector  $\mathbf{K}$  in the range 0–360° and determine the horizontal velocity modulus  $V_h(t)$  at each specific in-stant of time.

Afraimovich et al.(1998, 1999) described updating of the SADM algorithm for GPS-arrays (SADM-GPS) based on a simple model for the displacement of the phase interference pattern that travels without a change in the shape and on using current information about angular coordinates of the GPS satellites: the elevation  $\theta_s(t)$  and the azimuth  $\alpha_s(t)$ . Of course, such an approximation is acceptable only for large values of the LOS elevation  $\theta_s$ .

The method SADM-GPS permits to determine the horizontal velocity  $V_h(t)$  and the azimuth  $\alpha(t)$  of TID displacement at each specific in-stant of time (the wave-vector orientation  $\mathbf{K}$ ) in a fixed coordinate system  $(x, y)$ :

$$\begin{aligned}
\alpha(t) &= \arctan(u_y(t)/u_x(t)) \\
u_x(t) &= I'_t(t)/I'_x(t) = u(t)/\cos \alpha(t) \\
u_y(t) &= I'_t(t)/I'_y(t) = u(t)/\sin \alpha(t) \\
u(t) &= |u_x(t)u_y(t)|/(u_x^2(t) + u_y^2(t))^{-1/2} \\
V_x(t) &= u(t) \sin \alpha(t) + w_x(t) \\
V_y(t) &= u(t) \cos \alpha(t) + w_y(t) \\
V_h(t) &= (V_x^2(t) + V_y^2(t))^{1/2}
\end{aligned} \tag{9}$$

where  $u_x$  and  $u_y$  are the propagation velocities of the phase front along the axes  $x$  and  $y$  in a frame of reference related to the GPS-array;  $w_x$  and  $w_y$  are the  $x$  and  $y$  projections of the velocity  $w$  of the subionospheric point (for taking into account the motion of the satellite).

The coordinates of the subionospheric point  $x_s(t)$  and  $y_s(t)$  at  $h_{max}$  in the chosen topocentric coordinate system vary as:

$$\begin{aligned}
x_s(t) &= h_{max} \sin(\alpha_s(t)) \operatorname{ctg}(\theta_s(t)) \\
y_s(t) &= h_{max} \cos(\alpha_s(t)) \operatorname{ctg}(\theta_s(t))
\end{aligned} \tag{10}$$

and the  $x$ - and  $y$ - components of the displacement velocity  $w$ :

$$\begin{aligned}
w_x(t) &= d/dt(x_s(t)) \\
w_y(t) &= d/dt(y_s(t)) \\
w(t) &= (w_x^2(t) + w_y^2(t))^{1/2}
\end{aligned} \tag{11}$$

Let us take a brief look at the sequence of data handling procedures. Out of a large number of GPS stations, three points (A, B, C) are chosen

in such a way that the distances between them do not exceed about one-half the expected wavelength  $\Lambda$  of the disturbance. The point B is taken to be the center of a topocentric frame of reference. Such a configuration of the GPS receivers represents a GPS-array (or a GPS-interferometer) with a minimum of the necessary number of elements. In regions with a dense network of GPS-points, we can obtain a broad range of GPS-arrays of a different configuration, which furnishing a means of testing the data obtained for reliability; in this paper we have taken advantage of this possibility.

The input data include series of the vertical TEC  $I_A(t)$ ,  $I_B(t)$ ,  $I_C(t)$ , as well as corresponding series of values of the elevation  $\theta_s(t)$  and the azimuth  $\alpha_s(t)$  of the LOS.

Series of the values of the elevation  $\theta_s(t)$  and azimuth  $\alpha_s(t)$  of the LOS are used to determine the location of the subionospheric point, as well as to calculate the elevation  $\theta$  of the wave vector  $\mathbf{K}$  of the disturbance from the known azimuth  $\alpha$  (see formula (12)).

Since the distance between GPS-array elements (from several tens to a few hundred of kilometers) is much smaller than that to the GPS satellite (over 20000 km), the array geometry at the height near the main maximum of the  $F_2$ -layer is identical to that on the ground.

Linear transformations of the differences of the values of the filtered TEC ( $I_B - I_A$ ) and ( $I_B - I_C$ ) at the receiving points A, B and C are used to calculate the components of the TEC gradient  $I'_x$  and  $I'_y$  (Afraimovich et al., 1998). The time derivative of TEC  $I'_t$  is determined by differentiating  $I_B(t)$  at the point B.

The resulting series are used to calculate instantaneous values of the horizontal velocity  $V_h(t)$  and the azimuth  $\alpha(t)$  of TID propagation. Next, the series  $V_h(t)$  and  $\alpha(t)$  are put to a statistical treatment. This involves constructing distributions of the horizontal velocity  $P(V_h)$  and direction  $P(\alpha)$  which are analyzed to test the hypothesis of the existence of the preferred propagation direction. If such a direction does exist, then the corresponding distributions are used to calculate the mean value of the horizontal velocity  $\langle V_h \rangle$ , as well as the mean value of the azimuth  $\langle \alpha \rangle$  of TID propagation.

As a first approximation, the transionospheric sounding method is responsive only to TIDs with the wave vector  $\mathbf{K}$  perpendicular to the direction  $\mathbf{r}$  of the LOS. A corresponding condition for elevation  $\theta$  and azimuth  $\alpha$  has the form



$$\tan \theta = -\cos(\alpha_s - \alpha) / \tan \theta_s \quad (12)$$

Hence the phase velocity modulus  $V$  can be defined as

$$V = V_h \times \cos(\theta) \quad (13)$$

The aspect dependence (12) of the TEC disturbance amplitude is of significant importance for investigating wave disturbances. The condition (12) imposes a constraint on the number of LOS for which a reliable detection of TIDs at the background of noise is possible. The aspect effect causes the disturbance maximum to be displaced along the time axis, which can introduce errors in determining the TID displacement if the velocity is calculated from time delays. Furthermore, as will be shown below, the aspect effect will give rise to structures of the type of wave packets "observed" in TEC variations, which do not exist in the reality.

Afraimovich et al. (1992) showed that for the Gaussian ionization distribution the TEC disturbance amplitude  $M$  is determined by the aspect angle  $\gamma$  between the vectors  $\mathbf{K}$  and  $\mathbf{r}$ , as well as by the ratio of the wavelength of the disturbance  $\Lambda$  to the half-thickness of the ionization maximum  $h_d$ :

$$M(\gamma) \propto \frac{h_d}{\sin(\theta_s)} \cdot \exp \left[ - \left( \frac{\pi h_d \cos(\gamma)}{\Lambda \sin(\theta_s)} \right)^2 \right] \quad (14)$$

In this paper the influence of aspect effects on the character of TEC behavior and on the accuracy of the calculated parameters of TWPs was investigated and the reliability of the determination of TWPs characteristics was verified by modeling the wave disturbances of electron density for the observing conditions of October 18, 2001.

Thus, on the basis of using the transformations described in this section, for each of the GPS arrays chosen for the analysis we obtained the average (for the time interval of about 1-2 hours) values of the following TWPs parameters:  $\langle A_I \rangle$ , the amplitude of the TEC disturbance;  $\langle \alpha \rangle$  and  $\langle \theta \rangle$  – the azimuth and elevation of the wave vector  $\mathbf{K}$ ;  $\langle V_h \rangle$  and  $\langle V \rangle$  – the horizontal component and the phase velocity modulus, the contrast  $C$ , and the azimuth of a normal to the wave front  $\alpha_c$  from the method reported by Mercier (1986).

### 4.3 Dynamic characteristics of TWP

Fig. 7a plots the typical time dependencies of TEC  $I(t)$  for GPS satellite PRN14 for three GPS stations: BRAN, CHMS, and DUPS in California. The three GPS sites constitute a typical GPS array, the data from which were processed by the technique described in the preceding section. For the same stations Fig. 7b presents the TEC variations  $dI(t)$  that were filtered from the initial series  $I(t)$  using the band-pass filter with the boundaries from 5 to 20 min.

The filtered series for the period 15:00–16:00 UT show the presence of significant TEC pulsations of the type of single wave packet with a duration of about one hour and with the amplitude  $A = 0.5 \text{ TECU}$ . Not only does the range of the filtered oscillations  $dI(t)$  far exceed the error of phase measurements ( $10^{-3} \text{ TECU}$ ), but it also exceeds nearly an order of magnitude the level of background TEC variations. TEC variations from the three spatially separated GPS stations show a high degree of similarity and have a small time shift. This suggests that we are dealing here with the same traveling disturbance.

Results of a calculation (using the SADM-GPS algorithm) of the mean values of the azimuth  $\langle\alpha\rangle$  and the horizontal velocity  $\langle V_h\rangle$  of the disturbance for each 30-s time interval are presented in Fig. 7c and 7d. As is evident from the figure, this wave packet was traveling predominantly in the south-eastward direction with the mean velocity of about 180 m/s. The scatter of the counts is caused by the incomplete correspondence of the actual picture of an ideal TWP model in the form of a monochromatic packet (5) and, in particular, by the presence of background non-correlated TEC fluctuations (Afraimovich et al., 1998).

A processing of the data from the other GPS arrays in the same region (Fig. 4c) by use of the SADM-GPS method provided distributions of the main TWP parameters recorded on October 18, 2001 in California. The various combinations of GPS arrays for the time interval 15–16 UT totaled 231. Statistical data show an agreement of the mean values of the calculated parameters to within their standard deviations, which indicates a good stability of the data obtained, irrespective of the particular configuration of a GPS array.

Distributions of the mean values of the TWP parameters calculated for each of the 231 GPS arrays are presented in panels (a – c) of Fig. 8. Accord-

ing to our data, the value of the horizontal propagation velocity  $V_h$  of TWP (Fig. 8a) varies from 60 to 270 m/s, on the average, with the most probable value 190 m/s. The TWP wavelength  $\Lambda$  with the mean oscillation period of about 1000 s is on the order of 150–200 km.

An analysis of the distribution of the azimuths  $P(\alpha)$  (Fig. 8b) shows a clearly pronounced south-eastward direction of TWP displacement  $140 \pm 20^\circ$ . The average (for 231 GPS arrays) value of the contrast  $C = 7$  suggests a strong anisotropy of TWP. Fig. 8b shows also the distribution of the azimuth of a normal to the wave front  $P(\alpha_c)$  deduced by the method of Mercier (1986). This distribution virtually coincides with  $P(\alpha)$ , suggesting that the TWP travel across their elongation. Thus the typical size of the entire wave packet along the propagation direction is about 300–500 km, and along the wave front it is as long as 1000 m.

The arrow in Fig. 4c schematically shows the wave vector  $\mathbf{K}$  of the TWP. The values of  $\alpha$  and  $V_h$ , presented in Fig. 4c, correspond to the most probable values of the propagation azimuth and the modulus of the horizontal velocity of the TWP.

The elevation of the TWP wave vector, determined from the aspect condition (12), has mostly a small positive value (Fig. 8c): i.e. the oscillation phase propagates upward. Since the mean value of the elevation is only  $+10^\circ$ , it can be assumed that TEC pulsations represent an almost horizontal wave. Accordingly, estimations of the modulus of the phase velocity  $V$  (Fig. 8a) give values close to the value of its horizontal projection 50–270 m/s, with the largest probable value 180 m/s.

## 4.4 Modeling

In this paper the influence of aspect effects on the character of TEC behavior and on the accuracy of the calculated of TEC pulsations was investigated and the reliability of the determination of the TWP characteristics was verified by modeling the wave disturbances of electron density for the observing conditions of October 18, 2001.

Our developed model of TEC measurements with the GPS interferometer makes it possible to calculate as realistic a spatial and temporal distribution of the local electron density  $N_e$  in the ionosphere as possible and then, using the coordinates of the receiver sites and of the satellites, to integrate  $N_e$  along the receiver-satellite LOS with a given step over time (Afraimovich

et al., 1998). As a result we obtain time series of TEC similar to input experimental data which can be processed by the same methods as used to process experimental data.

The ionization model takes into account the height distribution of  $N_e$ , the seasonal and diurnal density variations determined by the zenith angle of the Sun, as well as irregular disturbances of  $N_e$  of a smaller amplitude and smaller spatial scales in the form of a discrete superposition of plane traveling waves.

In this paper, with the purpose of elucidating the origin of TWP, three types of disturbances were modeled:

a) the disturbance in the form of a single plane wave with amplitude  $A_1=3\%$  in the ionization maximum, with the period  $T_1=15$  min and the wavelength  $L_1=172$  km. The elevation of the wave  $\theta_1=10^\circ$ , and the azimuth  $\alpha_1=146^\circ$ ;

b) the disturbance in the form of a superposition of two plane waves with periods  $T_1=15$  min and  $T_2=12$  min, and with the wavelengths  $L_1=172$  km and  $L_2=138$  km. The elevations, azimuths and azimuths of the waves were specified identical:  $\theta_1=\theta_2=10^\circ$ ,  $\alpha_1=\alpha_2=146^\circ$ ,  $A_1=A_2=3\%$  of the value of  $N_e$  in the ionization maximum;

c) the disturbance in the form of a single wave packet, with the semi-thickness  $t_d=20$  min and a maximum amplitude at the time  $t_{max}=15.5$  UT. The oscillations inside the packet had the period  $T_1=15$  min and the wavelength  $L_1=172$  km.

Disturbance parameters were taken to be close to those obtained from experimental data using the technique from (Afraimovich et al., 1998). TEC pulsations were modeled with the purpose of (1) verifying the reliability of the calculated TWP characteristics, and (2) elucidating the origin of TWP. A detailed description of the model used is given in (Afraimovich et al., 1998).

Fig. 7 (panels **e–h** at the right) presents the results of calculations in terms of the model of the TWP in the form of a single wave packet for the BRAN, CHSM, DUPR array on October 18, 2001. Parameters of the wave packet were taken to be close to experimental data (Fig. 7a–d). Distributions of pulsation parameters obtained in a similar modeling of TWP for the other California GPS arrays are presented in Fig. 8 (panels **d–f** at the right).

Fig. 7 illustrates a good similarity of the experimental and model TEC variations  $I(t)$ ,  $dI(t)$  and the dependencies  $V_h(t)$  and  $\alpha(t)$ . Noteworthy is the weaker inclination of the model TEC  $I(t)$  (Fig. 7e) when compared with

the experimental one (Fig. 7a). This is because for the sake of simplicity and for illustrative purposes, diurnal variations in ionization in the model are proportional to the cosine of the zenith angle of the Sun. In actual conditions the dependence is more complicated, which gives a faster temporal growth of the TEC. because the trend is removed in the subsequent discussion and only the relative TEC variations  $dI(t)$  are considered, the above-mentioned difference in the behavior of the model and experimental TEC will not affect results obtained.

A comparison of the TEC disturbance parameters specified in the model with the corresponding values obtained following a processing by formulas of the SADM-GPS method shows a relatively good agreement of these values. The azimuth of the wave vector of TWP was taken to be  $\alpha = 146^\circ$ , and the mean value of the azimuth calculated by the SADM-GPS method is  $146.2^\circ$  (Fig. 7g, and Fig. 8e); the horizontal velocity was specified equal to 180 m/s, the calculated mean value of the velocity was 207.5 m/s (Fig. 7h, and Fig. 8d); the elevation in the model was  $\theta = 10^\circ$ , and the most probable value of the calculated elevation was  $10^\circ$  (Fig. 8f). The azimuth of TWP propagation determined by the SADM-GPS method was also close to the azimuth values calculated by analyzing the contrast of the phase interference pattern (Mercier, 1986) – Fig. 8b, e. All this demonstrates the validity of the SADM-GPS technique and confirms the reliability of the TWP parameters obtained using this technique.

Let us now consider the possible mechanisms that are responsible for the formation of structures of the type of pulsations in observed TEC variations. The recorded TEC pulsation represents a single wave packet with a duration of about 60 min, the oscillation period inside the packet of 12–15 min, and with the amplitude exceeding the level of background fluctuations by a factor of 2–5 (Fig. 7b). Structures of such a type can be produced in TEC variations in different ways.

If a monochromatic wave with a period of about 15 min (the period of observed TEC variations) propagates in the ionosphere, then TEC oscillations of the type of pulsations could be produced through the aspect effect. Fig. 9a, d illustrates such a situation. Panels **a** and **d** present the filtered TEC series obtained by modeling a single plane wave under different conditions of its observation. At the BRAN site (Fig. 9a) the elevations of the PRN14 satellite are close to  $90^\circ$ , and the wave vector of the disturbance is perpendicular to the receiver-satellite LOS throughout the observing period. This

is indicated by the character of the theoretical dependence  $M(\gamma)$  calculated by formula (14) for this LOS:  $M(\gamma)$  is close to 1 over the entire observing interval (Fig. 9c). Waves disturbances of the TEC close to the specified monochromatic wave are therefore observed along the BRAN–PRN14 LOS.

At the BRU1 site for PRN05, the detection conditions for disturbances are significantly worse. In this case for the first half an hour the wave propagates virtually along the LOS ( $M(\gamma) < 0.3$ , Fig. 9f), and at the end of the observing interval the BRU1–PRN15 LOS is perpendicular to the propagation direction of the wave but has low elevations ( $M(\gamma) > 1$ , Fig. 9f). Owing to this, TEC variations show an increase in the oscillation amplitude from 0 to 0.7 *TECU* – there arises a feature resembling a wave packet that was absent in the initial specified model of the wave. However, as is evident from the figure, in this case the increase in the TEC variation amplitude has an almost linear character while the experiment (Fig. 7b) shows a nonlinear amplitude modulation.

An investigation of the character of the aspect dependence for all GPS arrays that were used in this study, showed that in 97% of cases (including those shown in Fig. 7b) the situation is realized, which is depicted in Fig. 9c, i.e.  $M(\gamma)$  is close to 1 throughout this observing interval. Considering all that has been said above, one can draw the conclusion that the recorded TEC pulsations are indeed caused by the propagation of an actual wave packet of a local density disturbance in the ionosphere rather than resulting from the recording conditions.

Another possibility of the production of a TWP is the combination of two or several monochromatic waves with close periods propagating in the ionosphere (Yakovets et al., 1999). We modeled the propagation of two quasi-horizontal waves with periods  $T_1=15$  min and  $T_2=12$  min by identical amplitudes, velocities and directions of propagation. The resulting TEC variations along two LOS: BRAN–PRN14, and BRU1–PRN05, with the trend removed, are presented in Fig. 9b and 9e, respectively.

As would be expected, there arise amplitude-modulated TEC oscillations with the modulation period of about  $T = \frac{T_1 T_2}{T_2 - T_1} = 60$  min. The period is close to the length of the wave packet recorded experimentally; however, a simple superposition of two waves gives not one but a whole chain of wave packets. In the case where the aspect effect affects little the character of TEC variations (Fig. 9c) these packets have, in addition, different amplitudes as well (Fig. 9b). A phase change of the combined waves affects little the picture pre-

sented here by altering the form and position of the amplitude minimum only slightly. The aspect dependence in Fig. 9f, however, introduces an additional modulation into the recorded signal - there occurs a significant enhancement of one of the chain's packets (Fig. 9e), and the picture approaches what is observed experimentally in Fig. 7b.

Nevertheless, it cannot be believed that the observed single TWPs are the result of the aspect effect. Firstly, in the case of the aspect modulation, because of the slow(nearly linear) change of the amplitude, not one but at least two wave packets are observed. Secondly, as has been pointed out above, the character of the aspect dependence in most cases of TWP recordings was such that it affected little the amplitude of disturbances. To obtain the closest TEC oscillations to those observed experimentally we had to introduce an artificial modulation, i.e. the amplitude of the initial monochromatic wave of the disturbance  $N_e$  was specified not constant but it had a time dependence in the form of a Gaussian function. It is such a model of TEC variations that is shown in Fig. 7f.

## 5 Discussion of results

Sequences of wave packets similar to the ones shown in Fig. 6 at the left, were recorded in frequency Doppler variations with the multifrequency Doppler ionosonde at Almaty (Yakovets et al., 1999). The recordings of the frequency Doppler shift presented clearly show chains of wave packets (on the average, 2-3 wave packets with the record length of about 8 hours). The duration of the wave packets averaged 90 min, and the oscillation period in a packet averaged 16 min.

The authors of the cited reference observed two types of FD-variations: quasi-stochastic TIDs, and monochromatic TIDs in the form of wave packets. They concluded that quasi-stochastic TIDs are characterized by a random behavior of the phase, a small length of coherence, and by a large vertical phase velocity. Wave packets show quasi-monochromatic oscillations, a larger length of coherence, and a smaller vertical phase velocity.

Our estimate of the radius of spatial correlation (on the order of several hundred kilometers) is in reasonably good agreement with the data reported by Yakovets et al. (1995).

Yakovets et al. (1999) argued that the observed wave packets are the

superposition of the direct and ground-reflected wave whose source lies in the troposphere. The analysis made in this paper did not confirm the validity of such an explanation for the October 18, 2001 TWP.

By comparing our detected TEC pulsations with the data from (Yakovets et al., 1999; Hines, 1960; Waldock and Jones, 1984; Francis, 1974) as well as with the findings of our modeling, it can be assumed that in the atmosphere there exists an additional amplitude modulation mechanism for wave processes which make it possible to obtain TEC oscillations in the form of a single wave packet. Francis (1974), by considering the auroral electrojet to be the source of TIDs, showed that upon propagating through the atmosphere into the  $F$ -region, the ground-reflected waves acquire the properties of a wave packet. On the basis of the dispersion relation Hines (1960) and Waldock and Jones (1984) showed that TIDs that are associated with a tropospheric jet flow occur in the  $F$ -region in the form of a wave packet with quasi-monochromatic oscillations, the period of which is a function of inclination angle of the wave vector during the propagation of the wave from the source to the place of observation in the  $F$ -region.

Our data on the TWP displacement velocity and direction correspond to those of mid-latitude medium-scale traveling ionospheric disturbances (MS TIDs) obtained previously in the analysis of phase characteristics of HF radio signals (Kalikhman, 1980; Afraimovich, 1982; Waldock and Jones, 1984; 1986; 1987; Jacobson and Carlos, 1991), as well as signals from first-generation navigation satellites (Spoelstra, 1992), geostationary satellites (Afraimovich et al., 1997b; Jacobson et al., 1995) and discrete space radio sources (Mercier, 1986; 1996; Velthoven et al., 1990).

## 6 Conclusion

Main results of this study may be summarized as follows:

1. The most of the TWPs are observed during the daytime in no more than 0.1-0.4% of the total number of radio paths, most commonly in winter and autumn in a weakly disturbed or quiet geomagnetic situation. The distance between any two GPS stations where the TWPs within a single 2.3-hour time interval were observed does not exceed 500 km.



2. TWPs in the time range represent quasi-periodic oscillations of TEC of a length on the order of 1 hour with the oscillation period in the range 10–20 min and the amplitude exceeding the amplitude of "background" TEC fluctuations by one order of magnitude, as a minimum and is 0.3 *TECU*.
3. The dynamical parameters of the TWP observed on October 18, 2001 over California, USA were determined. The TWP traveled with the elevation  $\theta = 10^\circ$  and the azimuth  $\alpha = 146^\circ$ . Its mean velocity  $\langle V \rangle = 180$  m/c corresponds to the velocity of medium-scale AGW.
4. It is probably that TWP origins are medium-scale AGW.

## ACKNOWLEDGMENTS

We are indebted to Dr A.S. Potapov for participating in discussions. We thank O.S. Lesyuta for help in organizing the experiment. We are also grateful to V.G. Mikhalkovsky for his assistance in preparing the English version of the manuscript. This work was done with support under RFBR grant of leading scientific schools of the Russian Federation No. 00-15-98509 and INTAS grant No. 99-1186 as well as Russian Foundation for Basic Research grants No. 01-05-65374, 00-05-72026.

## References

- [1] Afraimovich E. L. Interference methods of ionospheric radio sounding. Moscow: Nauka, 1982, 198 p.
- [2] Afraimovich, E. L., A. I. Terekhov, M. Yu. Udodov, and S. V. Fridman, Refraction distortions of transionospheric radio signals caused by changes in a regular ionosphere and by travelling ionospheric disturbances, *J. Atmos. and Terr. Phys.*, 54, 1013–1020, 1992.
- [3] Afraimovich. E. L. Dynamics and anisotropy of traveling ionospheric disturbances as deduced from transionospheric sounding data. - Statistical angle-of-arrival and doppler method (SADM). Preprint ISTP, 1995, N5-95, 54p.

- [4] Afraimovich E. L. Statistical angle-of-arrival and doppler method (SADM) for determining characteristics of the dynamics of the transionospheric radio signal interference pattern. *Acta Geod. Geoph. Hung.*, 1997, V.32, N3-4, 461–468.
- [5] Afraimovich E. L., Boitman O. N., Zhovty E. I., Kalikhman A. D. and Pirog T. G. Dynamics and anisotropy of medium-scale traveling ionospheric disturbances as deduced from transionospheric sounding data. *Acta Geod. Geoph. Hung.*, 1997, V.32, N3-4, 301–308.
- [6] Afraimovich, E. L., K. S. Palamartchouk, and N. P. Perevalova, GPS radio interferometry of travelling ionospheric disturbances, *J. Atmos. and Solar-Terr. Phys.*, 60, 1205–1223, 1998.
- [7] Afraimovich, E. L., K. S. Palamartchouk, and N. P. Perevalova, Statistical angle-of-arrival and doppler method for GPS interferometry of TIDs, *Adv. of Space Res.*, 26, N6, 1001–1004, 2000.
- [8] Afraimovich E. L., Kosogorov E. A., Lesyuta O. S., Yakovets A. F., Ushakov I. I. Geomagnetic control of the spectrum of traveling ionospheric disturbances based on data from a global GPS network. *Ann. Geophys.*, 19, N 7, 723–731, 2001.
- [9] Baker D.M., and Davies K., F2-region acoustic waves from severe weather. *J. Atmos. Terr. Phys.* 31, 1345–1352, N 11, 1969.
- [10] Bertin F., Testud J., Kersley L., Medium scale gravity waves in the ionospheric F-region and their possible origin in weather diturbances. *Planet Space Sci.* 23, 493–, 1975.
- [11] Bertin F., Testud J., Kersley L. and Rees P.R., The meteorological jet stream as a source of medium scale gravity waves in the thermosphere: an experimental study. *J Atmos. Terr. Phys.* 40, 1161–1183, N 10–11, 1978.
- [12] Davies, K., *Ionospheric radio waves*. Blaisdell Publishing Company. A Division of Ginn and Company, Waltham, Massachusetts-Toronto-London, 1969.
- [13] Davies K. and J.E. Jones. Three-dimensional observations of traveling ionospheric disturbances. *J.Atmos.Terr.Phys.*, 33, 39–46, 1971.

- [14] Francis, S. H., A theory of medium-scale traveling ionospheric disturbances, *J. Geophys. Res.*, *79*, 5245, 1974.
- [15] Gurtner, W. (1993) RINEX: The Receiver Independent Exchange Format Version 2. <http://igsceb.jpl.nasa.gov:80/igsceb/data/format/rinex2.txt>.
- [16] Hines, C. O., Internal atmospheric gravity waves at ionospheric heights, *Can. J. Phys.*, *38*, 1441, 1960.
- [17] Hines, C. O. and Reddy, C. A. On the Propagation of Atmospheric Gravity Waves through Regions of Wind Shear. *J. Geophys. Res.* **72**, 1015-1034, 1967.
- [18] Hocke, K., and K. Schlegel, A review of atmospheric gravity waves and traveling ionospheric disturbances: 1982-1995, *Ann. Geophys.*, *14*, 917-940, 1996.
- [19] Hofmann-Wellenhof, B., H. Lichtenegger, and J. Collins, Global Positioning System: Theory and Practice, Springer-Verlag Wien, New York, 1992.
- [20] Hung R.G., T. Phan, and R.E. Smith, Observation of gravity waves during the extreme tronodo outbreak of 3 April 1974, *J. Atmos. Terr. Phys.*, *40*, 831-, 1978.
- [21] Huang Yinn-Nien, Cheng Kang, and Sen-Wen Chen. On the detection of acoustic-gravity waves generated by typhon by use of real time HF Doppler frequency shift sounding system, *Radio sc.*, *20*, *N4*, 897-906, 1985.
- [22] Jacobson, A.R., R.C. Carlos. A study of apparent ionospheric motions associated with multiple travelling ionospheric disturbances. *J. Atm. Terr.Phys.*, *53*, 53-62, 1991.
- [23] Jacobson, A. R., R. C. Carlos, R. S. Massey, and G. Wu, Observations of traveling ionospheric disturbances with a satellite-beacon radio interferometer: Seasonal and local time behavior, *J. Geophys. Res.*, *100*, 1653-1665, 1995.
- [24] Kalikhman A. D. Medium-scale traveling ionospheric disturbances and thermospheric winds in the F-region. *J. Atmos. Sol. Terr. Phys.*, *42*, 697-703, 1980.

- [25] Kersly L. and Rees P.R., Tropospheric gravity waves and their possible association with medium-scale travelling ionospheric disturbances. *J. Atmos. Terr. Phys.* *44*, 147–, 1982.
- [26] Klobuchar, J. A., Ionospheric time-delay algorithm for single-frequency GPS users, *IEEE Transactions on Aerospace and Electronics System*, *AES 23(3)*, 325–331, 1986.
- [27] Mannucci A. J., Ho C. M., Lindqwister U. J. et al. A global mapping technique for GPS-driven ionospheric TEC measurements, *Radio Science*, *33*, 565–582, 1998.
- [28] Mercier, C. Observations atmospheric gravity waves by radiointerferometry, *J. Atmos. and Terr. Phys.*, *48*, 605–624, 1986.
- [29] Mercier, C., Some characteristics of atmospheric gravity waves observed by radio-interferometry, *Ann. Geophys.*, *14*, 42–58, 1996.
- [30] Oliver, W. L., Otsuka Y., Sato M., Takami T., and Fukao, S. A climatology of F region gravity waves propagation over the middle and upper atmosphere radar. *J. Geophys. Res.* **102**, 14449-14512, 1997.
- [31] Spoelstra, T. A. Th. Combining TIDs observations: NNSS and radio interferometry data. *J. Atmos. Terr. Phys.*, *54*, 1185–1195, 1992.
- [32] Stobie J.G., Einaudi F. and Uccellini L.W., A Case Study of Gravity Waves-Cunvective Storms Interaction: 9 May 1979. *J. Atmos. Sci.* *40*, 2804–, 1983.
- [33] Velthoven, P.F.J., C. Mercier, and H. Kelder, Simultaneous observations of travelling ionospheric disturbances by twodimensional radio interferometry and the differential Doppler technique applied to satellite signals, *J. Atmos. Terr. Phys.*, *52*, 305–312, 1990.
- [34] Waldock, J. A., and T. B. Jones, The effect neutral winds on the propagation of medium-scale atmospheric gravity waves at mid-latitudes, *J. Atmos. and Terr. Phys.*, *46*, 217, 1984.
- [35] Waldock, J. A., and T. B. Jones, HF Doppler observations of medium-scale traveling ionospheric disturbances at mid-latitudes, *J. Atmos. Sol. Terr. Phys.*, *48*, 245–260, 1986.

- [36] Waldock J.A. and T.B. Jones. Source regions of medium-scale travelling ionospheric disturbances observed at mid-latitudes. *J. Atmos.Terr.Phys.*, *49*, 105–114, 1987.
- [37] Yakovets, A.F., M. Z. Kaliev, and V. V. Vodyannikov, An experimental study of wave packets in travelling ionospheric disturbances, *J. Atmos. and Terr. Phys.*, *45*, 629, 1999.

15.07.2001

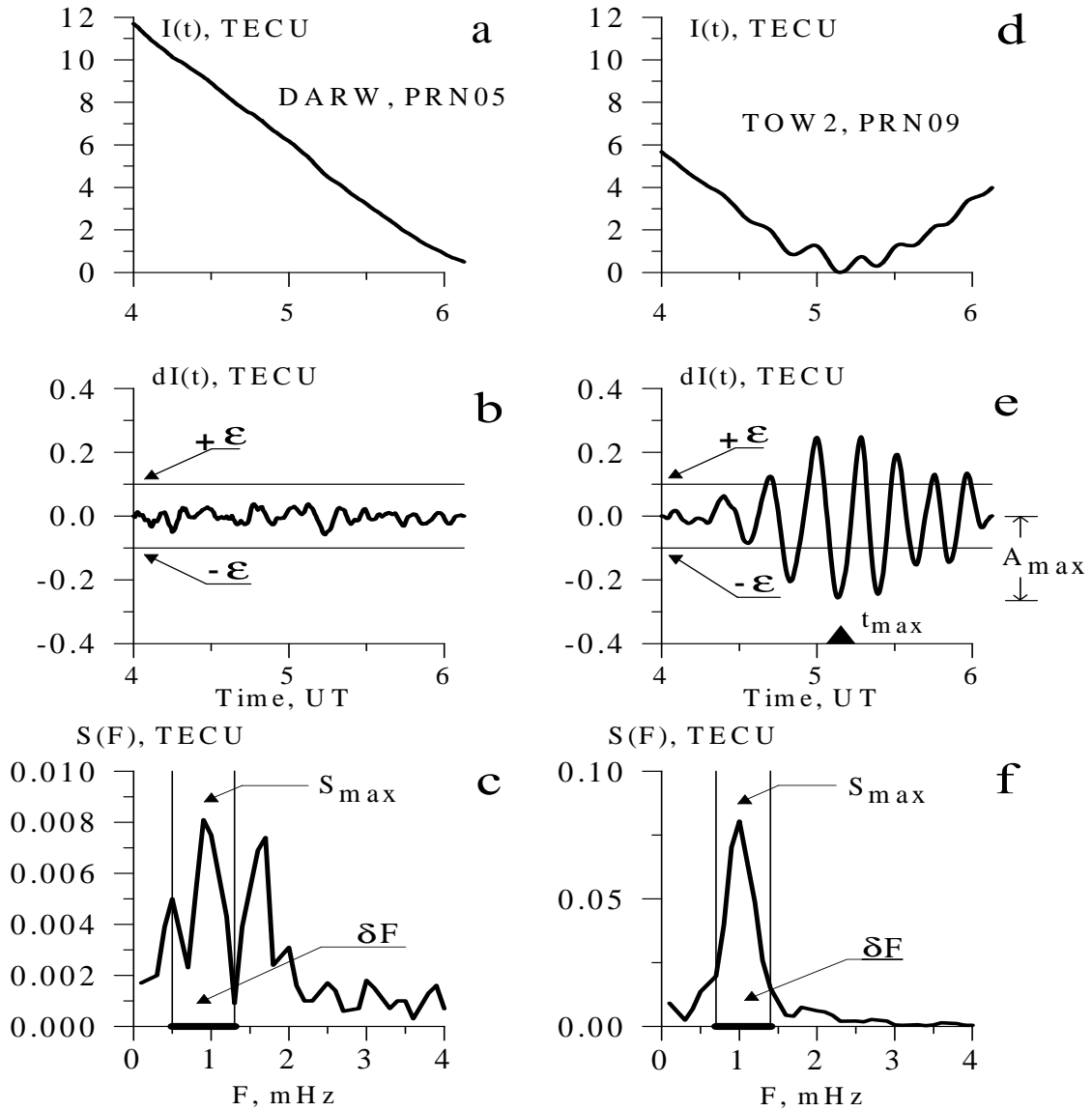


Figure 1: An illustration of the selection of TWPs: **a** – typical  $I(t)$  series containing no TWP; **b** and **c** – filtered  $dI(t)$ -series and its spectrum  $S(F)$ . Panels **d**, **e** and **f** – same but for the  $I(t)$ -series containing TWP. Shown in panels **a** and **d** are the station names and GPS satellite numbers. Levels of limitation in TWP amplitude  $\epsilon$  are shown in panels **b** and **e** by horizontal lines. Boundaries of the range of frequencies  $\delta F$  used in the analysis are shown in panels **c** and **f** by vertical lines. Panel **e** shows the maximum value of the amplitude  $A_{max}$  and the time  $t_{max}$  corresponding to this amplitude. The arrows in panels **c** and **f** indicate the maximum values of the amplitude spectra  $S_{max}$ .

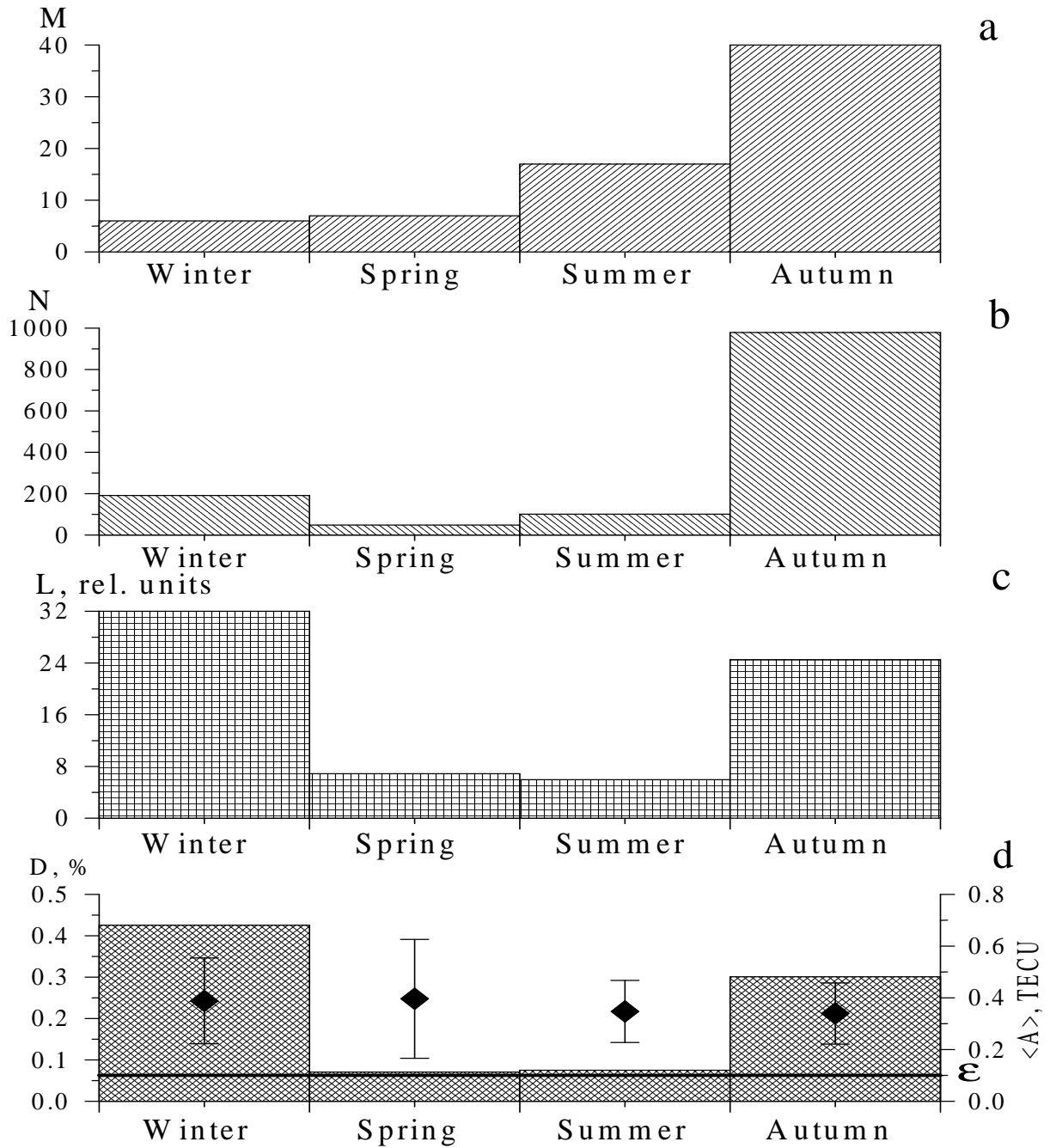


Figure 2: Seasonal dependence of the density and maximum amplitude of TWPs: **a** – number of days  $M$  of observation versus time of the year; **b** – number of TWPs  $N$ ; **c** – mean number of TWPs per day  $L = N/M$ . **d** – relative TWP density  $D$  obtained as the ratio of the number of TWPs  $N$  to the number of receiver-satellite LOS. Diamonds in panel **d** show the mean values of  $\langle A \rangle$  of the maximum amplitudes  $A_{max}$  for each season, and vertical lines show their standard deviations. The thick horizontal line shows the threshold in amplitude ( $\epsilon = 0.1$  TECU).

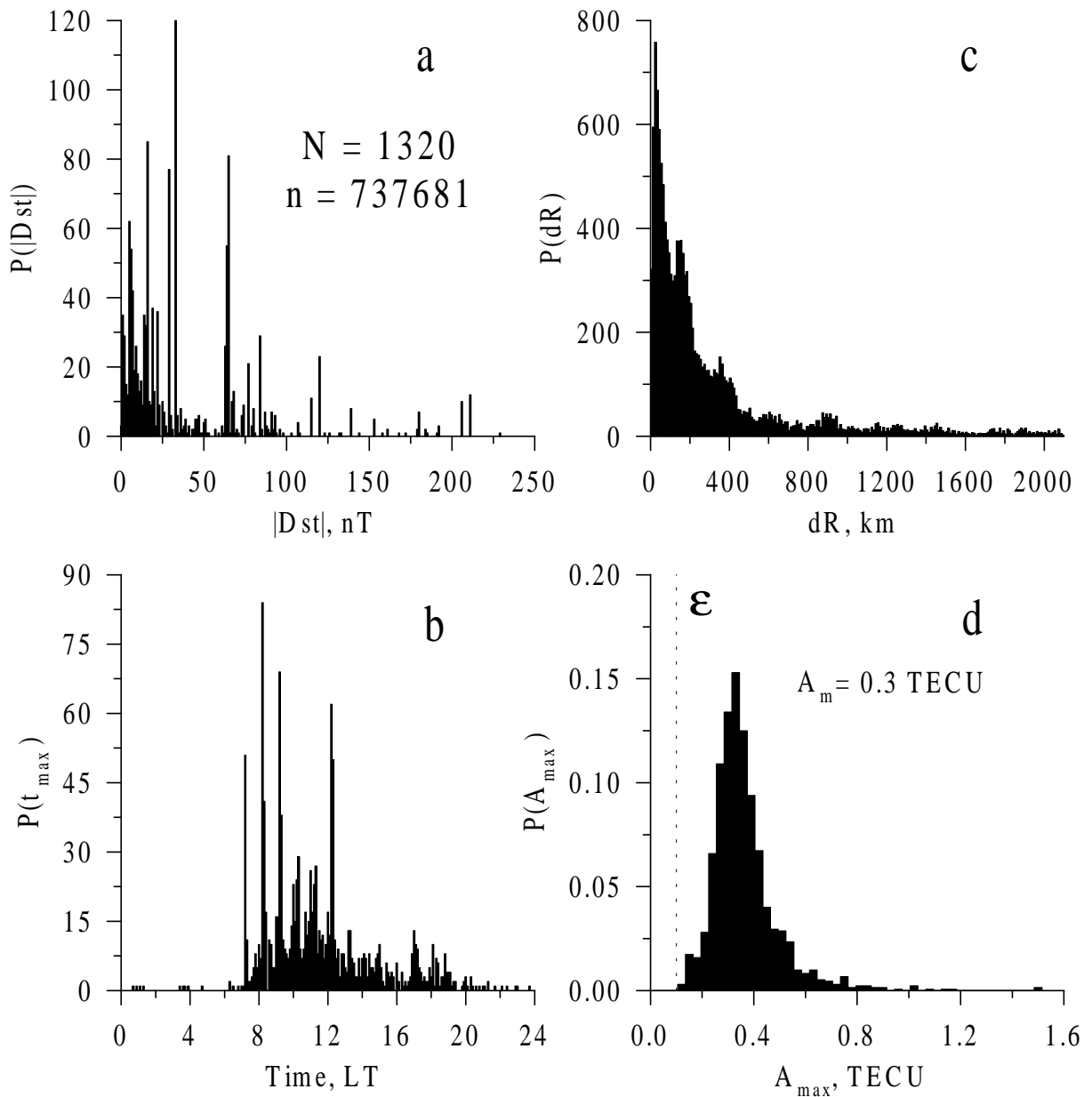


Figure 3: Statistic of TWPs: **a** – dependence of the number of TWPs on the modulus of the  $Dst$ -index; **b** – diurnal distribution  $P(t_{max})$  of the times  $t_{max}$  corresponding to the maximum amplitude  $A_{max}$  of the wave packet of the TEC disturbance; **c** – histogram  $P(dR)$  of the number of cases where TWPs within one 2.3-hour time interval were observed at any two GPS stations, with the distance  $dR$  between them; **d** – distribution  $P(A_{max})$  of the maximum amplitude  $A_{max}$  of TWP. The vertical dashed line in panel **d** shows the threshold in amplitude  $\epsilon = 0.1$  TECU. Panel **a** shows the number  $N$  of the detected TWPs, and the total number  $n$  of receiver-satellite LOS. Panel **d** shows the most probable maximum amplitude  $A_m$ .



This figure "fig4.jpg" is available in "jpg" format from:

<http://arxiv.org/ps/physics/0211046v1>

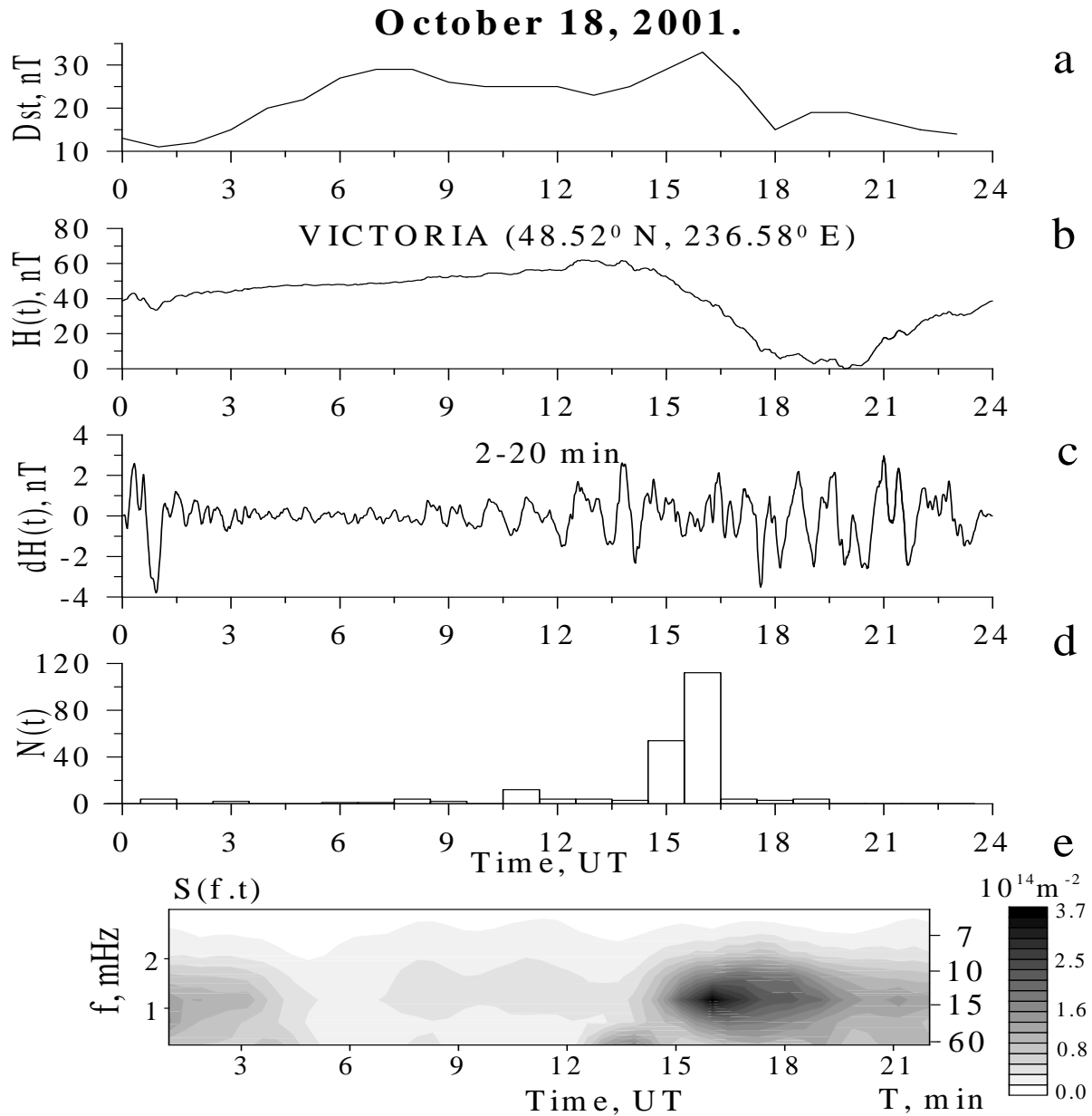


Figure 5: Geomagnetic field  $D_{st}$ -variations (a) October 18, 2001.  $H(t)$ -variations of the horizontal component of the geomagnetic field as recorded at station Victoria ( $236.58^{\circ} E$ ;  $48.52^{\circ} N$ ) – b.  $dH(t)$ -variations of the horizontal component of the geomagnetic field, filtered from the series  $H(t)$  in the range of periods of 2–20 min – c. d – distribution  $N(t)$  of the number of TWP detected on that day for all stations of the global GPS network used in the analysis, with the standard deviation higher than  $\epsilon = 0.1$  TECU; e – dynamic amplitude spectrum of TEC variations in the range of periods of 5–60 min obtained through a spatial averaging of the spectra for the entire California region ( $220$ – $260^{\circ} E$ ;  $28$ – $42^{\circ} N$ ).

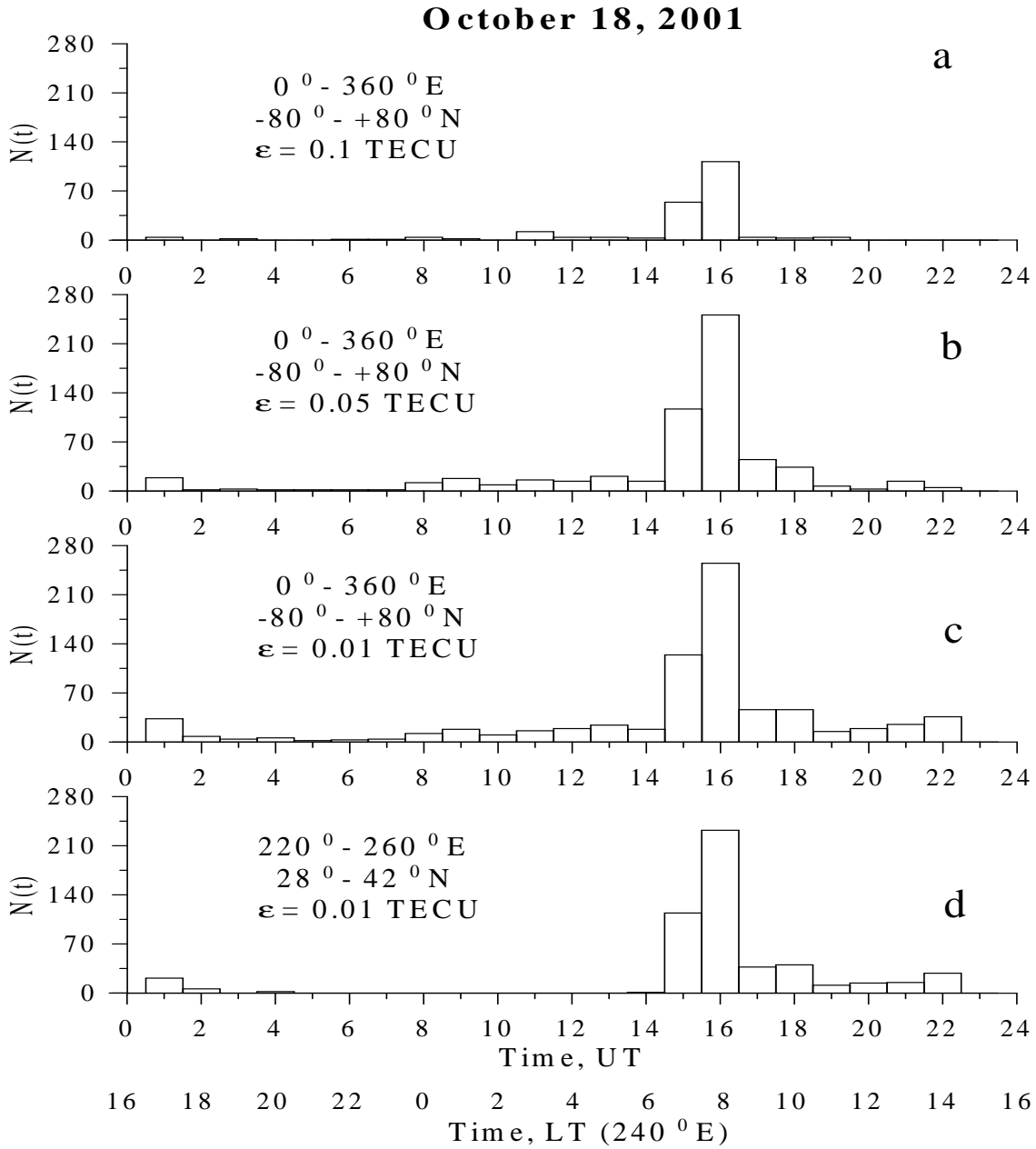


Figure 6: Number  $N(t)$  of TWP of October 18, 2001 as a function of UT and local time LT, calculated for the longitude of  $240^{\circ} E$ , corresponding to the middle of the California region: **a** – from TWPs with the standard deviation higher than  $\epsilon = 0.1 \text{ TECU}$  obtained for all stations of the global GPS network used in the analysis (copy of Fig. 5d); **b** and **c** – same as in a but for  $\epsilon = 0.05 \text{ TECU}$ , and  $\epsilon = 0.01 \text{ TECU}$ ; **d** – with the standard deviation higher than  $\epsilon = 0.01 \text{ TECU}$  according to the data from the California region only ( $220\text{--}260^{\circ} E$ ;  $28\text{--}42^{\circ} N$ ).

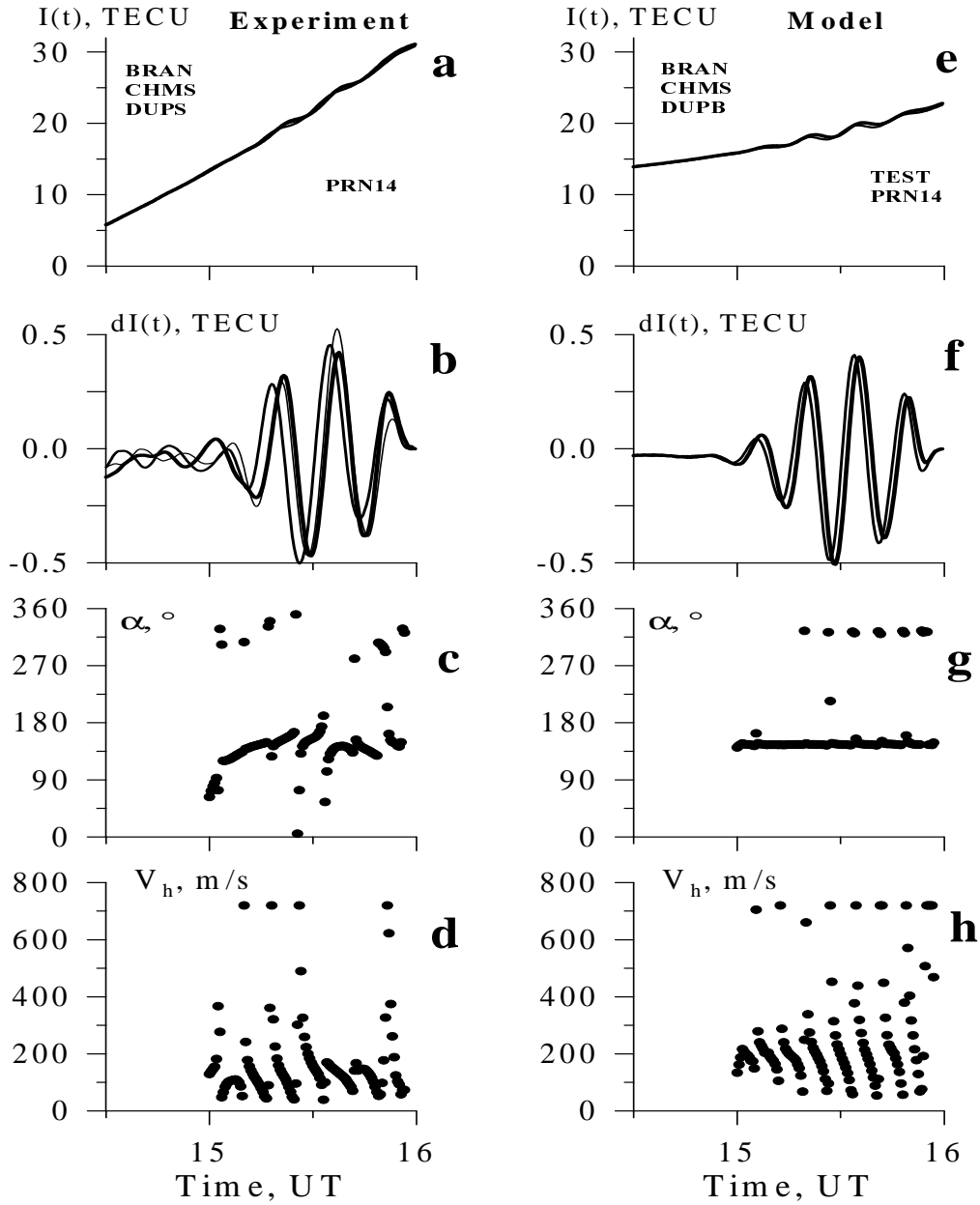


Figure 7: Time dependencies of the initial  $I(t)$  – panels **a**, **e** and filtered  $dI(t)$  – **b**, **f** TEC series; directions  $\alpha$  of the wave vector  $K$  – **c**, **g** and of the modulus of the vertical velocity  $V_h$  of TWP – **d**, **h**, determined for the GPS array (BRAN, CHMS, DUPS) using the SADM-GPS method. Panels **a** – **d** present the experimental data, and panels **e** – **h** show the calculated data for the TWP model in the form of a single wave packet.

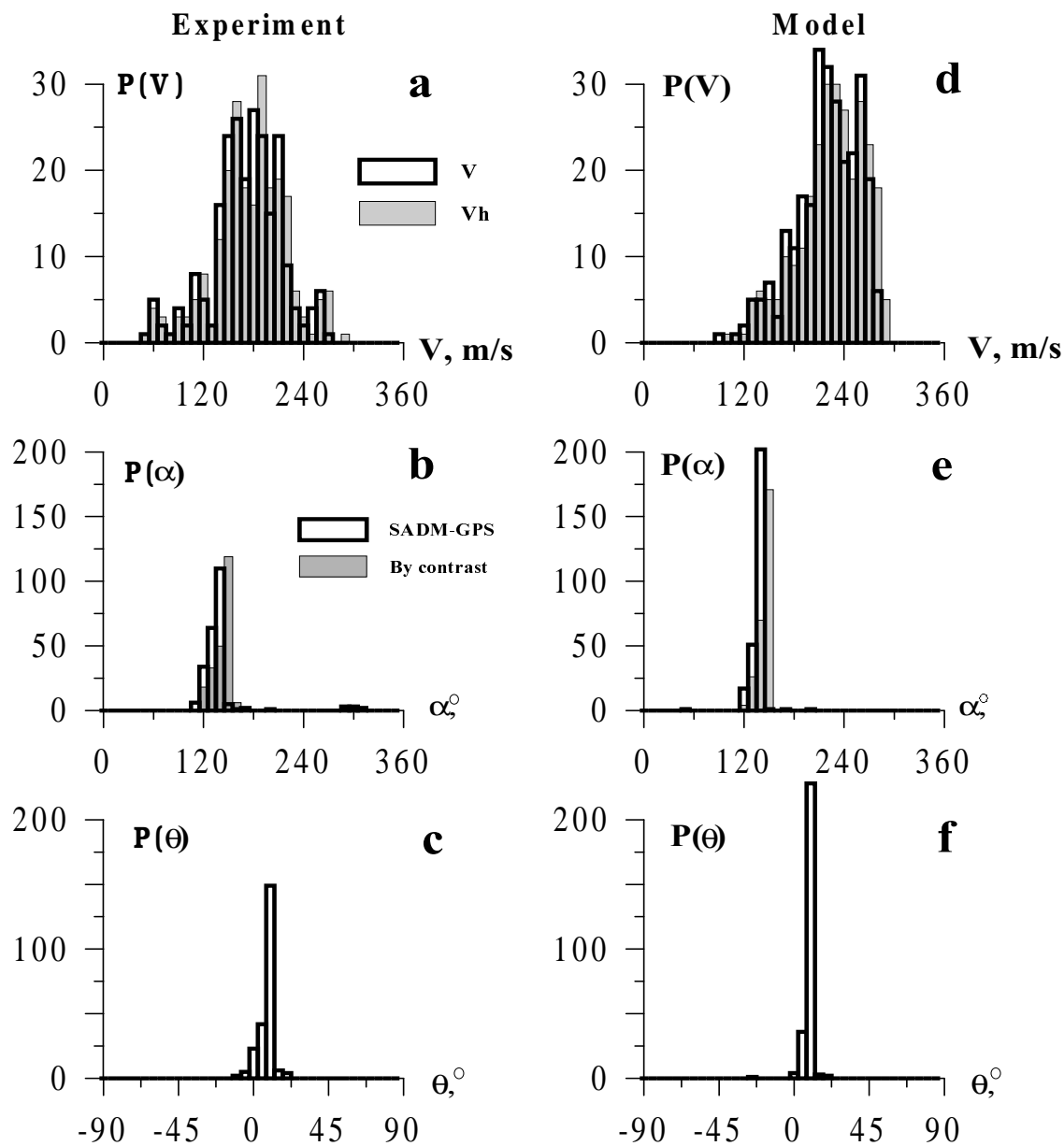


Figure 8: Distributions of the TWP parameters as determined by the SADM-GPS method: **a, d** – modulus (line 1) and horizontal component (line 2) of the TWP phase velocity; **b, e** – azimuth (line 1); **c, f** – elevation of the TWP wave vector. Panels **b** and **e** present also the distributions of the TWP propagation azimuth calculated from the contrast (line 2). Panels **a** – **c** present the experimental data, and panels **d** – **f** show the calculated data for the TWP model in the form of a single wave packet.

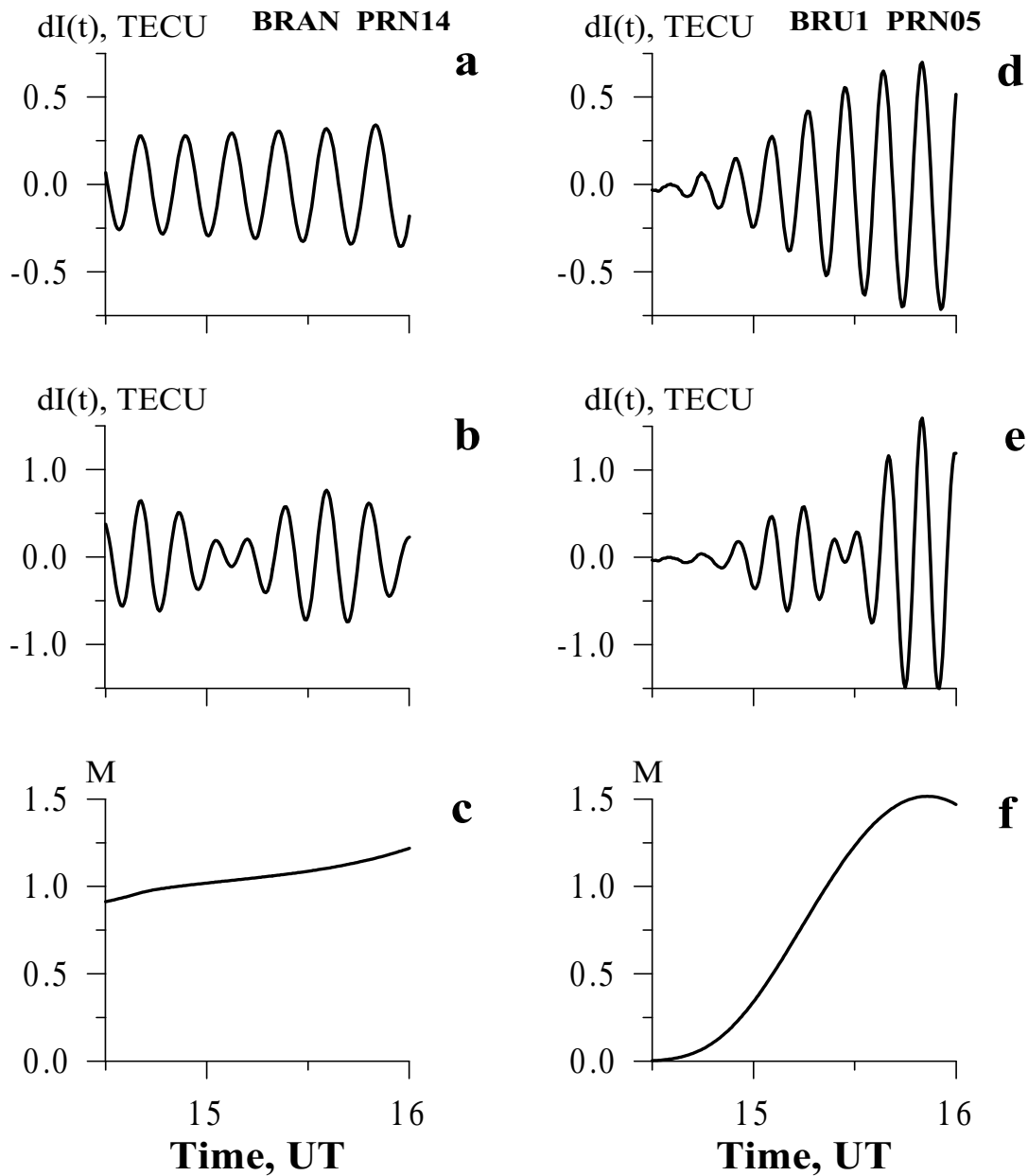


Figure 9: Time dependencies of the filtered  $dI(t)$  TEC series, calculated for the TID model in the form of a single plane wave (**a**, **d**) and in the form of a superposition of two plane waves (**b**, **e**). Panels (**c**, **f**) present the theoretical dependencies of the TEC response amplitude  $M(t)$ . On the left – calculations for the GPS PRN14 satellite at the BRAN site; on the right – for the PRN05 satellite at the BRU1 site.